Normal shock wave/turbulent boundary-layer interaction control using 'smart' piezoelectric actuators

J. S. Couldrick, S. L. Gai, J. F. Milthorpe and K. Shankar
School of Aerospace & Mechanical Engineering, University College, UNSW,
Australian Defence Force Academy,
Canberra, Australia

ABSTRACT

This paper looks at active control of the normal shock wave/turbulent boundary layer interaction (SBLI) using smart flap actuators. The actuators are manufactured by bonding piezoelectric material to an inert substrate to control the bleed/suction rate through a plenum chamber. The cavity allows rapid thickening of the boundary-layer approaching the shock, which splits into a series of weaker shocks forming a lambda shock foot, thus reducing wave drag. Active control allows optimisation of the interaction, as it would be capable of either positioning the control region around the original shock position using a series of unimorph flaps or fixing the shock position by controlling the rate of mass transfer.

The level of control achieved by unimorph piezoelectric actuators is not large because of small amounts of deflection possible. It is believed that to provide optimal control a piezoelectric material, which can provide greater strain and hence higher amounts of deflection is needed. However, currently such a piezoelectric material is not commercially available.

NOMENCLATURE

E	Young's Modulus
M	Mach number
R	reattachment
S	separation
t	thickness
x	normalised substrate thickness ($x = t_s/t_{pzt}$)
X	streamwise co-ordinate, mm
y	normalised Young's Modulus ($y = E_s/E_{pzt}$)
Y	vertical co-ordinate, mm
Z	spanwise co-ordinate, mm

Subscripts

n	normal
pzt	piezoceramic properties
s	substrate properties

Abbreviations

ACSBLI	active control of SBLI
EDM	electro discharge machining
FEM	finite element modelling
PCSBLI	passive control of SBLI
PZT	lead zirconate titanate
SBLI	shock wave/boundary-layer interaction
ANSYS®	proprietary name for a FEM programme

1.0 INTRODUCTION

For very weak shock waves, such as with an upstream Mach number of around 1·1, the extent of the shock wave/boundary-layer interaction is relatively weak, allowing the normal shock wave to extend into the boundary layer virtually as far as the sonic line with little smearing[1,2]. However, as the upstream Mach number increases, the distortion of the shock foot due to boundary-layer thickening becomes increasingly significant. Above a Mach number of approximately 1·3 separation first occurs and the shock wave foot bifurcates above the boundary layer to form a lambda (λ) foot, underneath which a small separation bubble occurs[3-6]. This is the so called incipient separation. The leading shock is usually highly oblique with the trailing part of the lambda foot nearly normal.

Paper No. 2940. Received on 14 November 2004, revised copy received on 22 June 2005, accepted 25 August 2005.
This paper was first presented at the RAeS Aerospace Aerodynamics Research Conference, September 2004.

https://doi.org/10.1017/S0001924000000919 Published online by Cambridge University Press

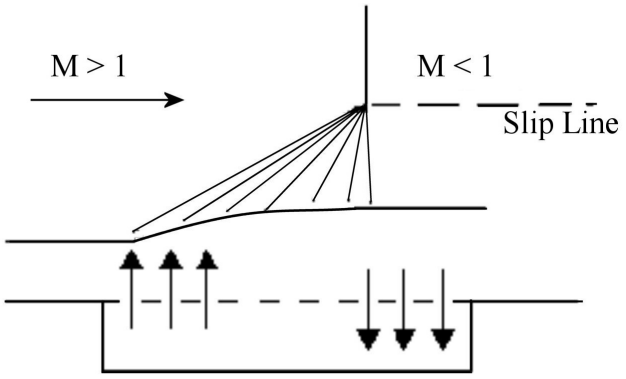


Figure 1. Passive control of the shock wave/boundary-layer interaction (PCSBLI).

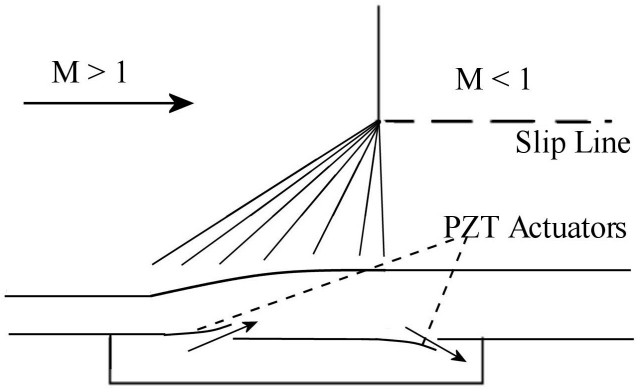


Figure 2. Active control of the shock wave/boundary-layer interaction (ACSBLI) using flap actuators.

Previous work[7-16] has been to passively control the interaction by replacing the surface beneath the foot of the shock wave with a porous plate covering a plenum chamber (Fig. 1). This allows high-pressure fluid from the flow downstream of the shock wave to re-circulate through the plenum chamber into the low-pressure flow upstream of the shock wave. Recirculation through the cavity allows rapid thickening of the boundary layer approaching the shock, which splits into a series of weaker shocks forming a lambda shock foot, reducing wave drag. Furthermore, the suction down-stream reduces separation and viscous losses. However, the beneficial effects are outbalanced by the additional friction drag produced by the 'rough' porous surface.

Historically, active control of the shock/boundary-layer interaction (ACSBLI), although effective, has been hampered by the drag reduction achieved being negated by the additional drag due to the power requirements, for example, the pumping power in the case of mass transfer. The object of the present research[17-20] is to assess the concept of active control using 'smart' flap actuators† (Fig. 2). The actuators are designed using PZT-5H piezoelectric material (PZT) to control bleed/suction rate. The previous work by the authors has only examined swept normal SBLI control and this paper presents the first results of unswept normal SBLI control using the piezoelectric actuators.

The plenum chamber pressure would approximately be at a mean value of the upstream and downstream pressure. Using this assumption, the pressure difference acting on the actuator will, therefore, be the difference between the chamber pressure and the free-stream pressure.

As active control should be capable of controlling the rate of mass transfer, a number of design options were considered for the integration of the PZT into the structure. These included the use of unimorph actuators with the PZT attached to one side of an inert substrate, bimorph actuators with two opposite poled PZT layers attached to each other to create twice the deflection and finally polymorphs with numerous PZT layers to further improve deflection characteristics. Furthermore, both bimorphs and polymorphs can be directly employed as actuators. However, the present paper describes actuators only of the unimorph variety to control normal SBLI. It should be reiterated that the present work does not include a closed loop system and the term active control using 'smart' piezoelectric flap actuators is mainly used to signify that the magnitude of unimorph deflection, and therefore level of SBLI control, can be managed.

†The term 'smart' in the present control is used in a very broad sense implying that piezoelectric actuators can either be activated to control the recirculation rate or can be 'switched off' leaving the recirculation rate uncontrolled.

2.0 EXPERIMENTAL ARRANGEMENT

The work was carried out in Tunnel 2, a blow-down supersonic wind tunnel, at the Engineering Department of The University of Cambridge at a Mach number of 1·5. The tunnel arrangement and control region are shown in Fig. 3(a). The working section is 114mm wide, 178mm high and the control plate on the floor is 172mm long. Manual adjustment of the stagnation pressure, along with a second

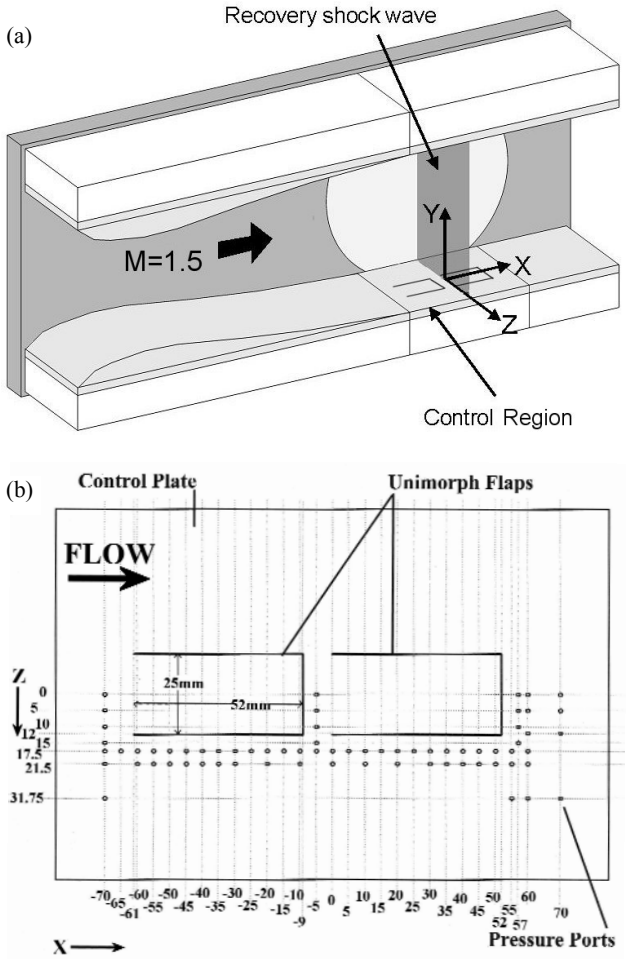


Figure 3. (a) The wind tunnel arrangement and (b) the pressure port layout on the control plate above the plenum chamber.

https://doi.org/10.1017/S0001924000000919 Published online by Cambridge University Press

throat, allows the recovery shock to be held at any given location. Three shock positions were investigated at approximately ⅓, ½ and ⅔ of the way along the control region. However, this paper concentrates on the middle shock position, which corresponds to $X = 0$ or the start of the downstream unimorph flap position (Fig 3b). The experiments made use of the interaction between the normal recovery shock and the naturally grown turbulent boundary layer on the tunnel floor with a unit Reynolds number of 23·65 * $10^6 m^{-1}$. The incoming boundary layer and displacement thicknesses at the control plate are approximately 7·54mm and 1·46mm respectively. For a test section static pressure of 41kPa the smart flaps will then have approximately 30kPa pressure difference acting across them.

A plenum chamber, 38mm in depth, is placed underneath the control plate in the floor of the test section. The plenum is covered by the control plate, containing the 'flaps' and numerous pressure ports, (Fig. 3b). The flaps were cut into the plate by electro discharge machining (EDM), with a gap of 0·2mm between the model skin and the flap. The gaps produced can be considered as providing continual passive slot control of the SBLI. The 'slots' are longitudinal and lateral in nature for the unimorph edges and ends respectively. The piezo-ceramic is bonded to the underside of the flap and a voltage is applied to control the actuator deflection and thus mass transfer rate. The surface pressure measurements were recorded using Druck PDCR-200 miniature pressure transducers connected to the pressure ports. Boundary layer traverses were performed downstream of the interaction using a flat head Pitot probe (dimensions 1·61mm × 0·131mm) connected to a pressure transducer. Surface oil flow visualisation was performed using a paraffin, titanium dioxide and oleic acid mixture.

The experimental errors in the surface static and pitot pressures measured using the transducers are of the order of 1%. The traverse gear used to measure the boundary-layer profile has accuracy better than 0·1mm (0·5% boundary layer thickness). A degree of unsteadiness was observed in the shock resulting in an error in the stream wise location of the order of 4mm (3·5% control region).

3.0 STRUCTURAL ASPECTS OF THE UNIMORPH ACTUATOR

3.1 Configuration

The concept for the unimorph set-up was to have the piezoceramic embedded within the surface material, (Fig. 4), to allow a greater bonding area and improved deflection properties, whilst retaining a flush upper surface. A lip was then incorporated into the design to minimise the deflection required before mass transfer occurred.

The tip deflection varies with the substrates' Young's Modulus and thickness[21]. The selection of substrate is a trade-off between suppressing the deflection due to the pressure difference across the flap, while keeping the unimorph electrically responsive to provide active control. Active control of the shock boundary-layer interaction requires that the flaps are able to close, have zero deflection, and minimum mass transfer. This trade-off restricts the substrate to a Young's Modulus similar to that of the piezoceramic, giving aluminium as a suitable substrate material. It was hoped to achieve better piezoelectric performance in testing, than theory suggests, due to the assumption of a constant mean pressure within the plenum chamber. In reality, there will be a pressure gradient in the plenum and spillage around the side edges, which will reduce the pressure acting on the flaps.

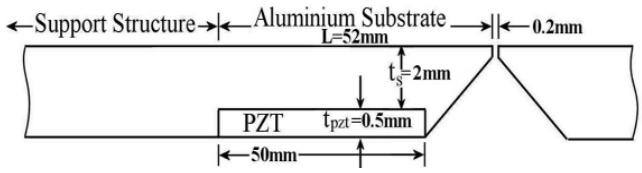


Figure 4. Modified unimorph flap configuration.

3.2 Finite Element Modelling (FEM)

ANSYS® v6.0† was utilised as the FEM program with a parametric design language program modelling the unimorph flap, supporting structure and solid substrate tip. Furthermore, it allowed analysis of complex pressure loadings, which satisfy aerodynamic boundary conditions.

The programme was able to predict the unimorph tip deflection under a quadratic pressure load of 30kPa, a value halfway between the theoretical upstream and downstream pressures. A ±500V applied voltage limit is used, which produces a ±1kVmm^{-1} field across the PZT, the materials applied field limit. With a 500V and –500V applied voltage inhibiting and assisting the unimorph flap deflection respectively.

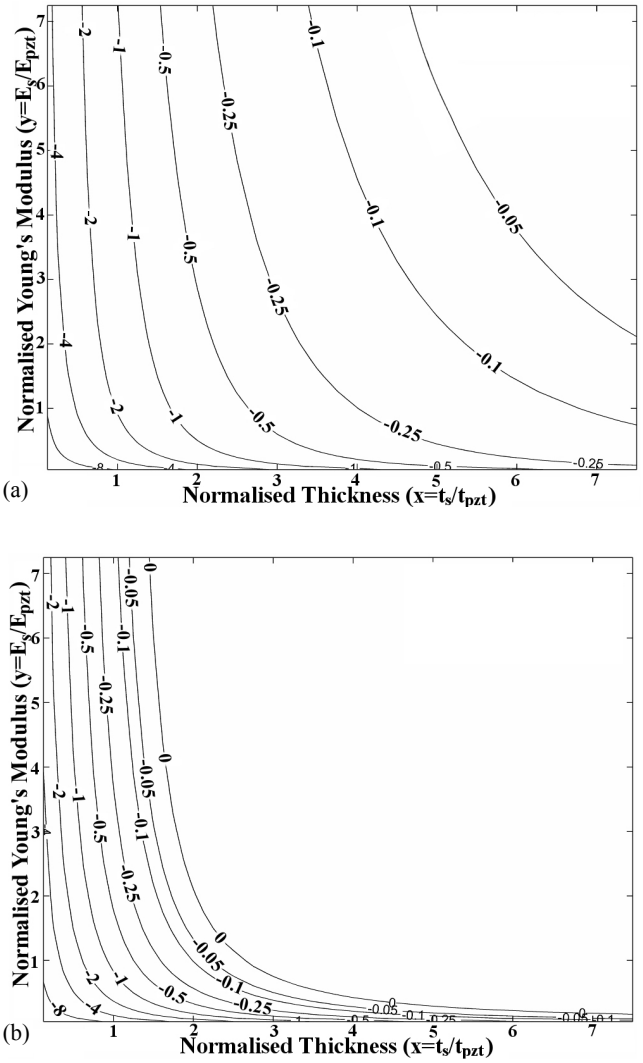


Figure 5. Contours of unimorph tip deflection (mm) with a quadratic pressure load, for applied fields of (a) –500V and (b) 500V.

† ANSYS® is a proprietary name for a FEM programme by ANSYS, inc.

https://doi.org/10.1017/S0001924000000919 Published online by Cambridge University Press

The FEM computations show that if the unimorph has to be capable of zero deflection to provide active control then for a 500V limit an aluminium substrate thickness has to be at least 1·25mm (x = 2·5). The final unimorph design used an aluminium substrate thickness of 2mm. The FEM computations gave the magnitude of maximum tip deflection as 0·24mm whilst ensuring closure and allowing the flap to be manufactured relatively flat, (Figs 5(a) & (b)).

4.0 RESULTS AND DISCUSSION

4.1. Zero deflection

Referring to Fig. 6(a), the flow is from left to right, with the normal shock, M_n = 1·5, interacting with the naturally grown boundary layer

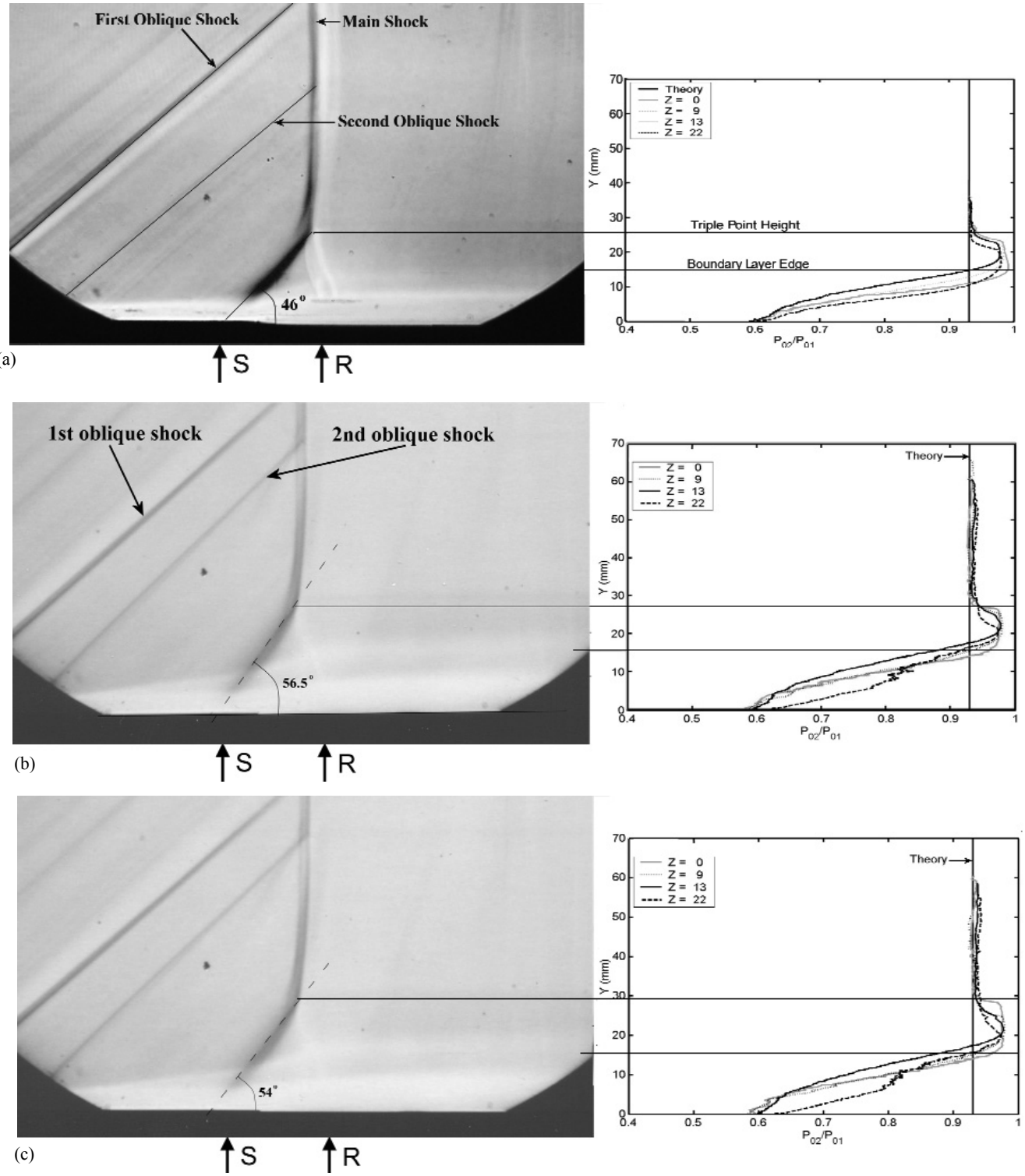


Figure 6. Schlieren pictures and total pressure traverses of the SBLI with unimorph control with (a) zero deflection, (b) 'closed flaps' (+500V) and (c) 'open flaps' (–500V).

https://doi.org/10.1017/S0001924000000919 Published online by Cambridge University Press

on the tunnel floor. The unimorph flaps have been fixed at zero deflection to observe passive control effects, if any, produced from the 'slots' arising from the way the flaps are manufactured, as mentioned in the experimental arrangement. From oil flow pictures it was observed that the flow has separated, as shown by separation (S) and reattachment (R) points.

Imperfections in the tunnel and the presence of pressure ports have caused spurious Mach waves upstream of the SBLI but these have negligible effect on the flow before the interaction.

Figures 6(a) – (c) have similar upstream oblique shocks that originate from the start of the test section control plate and are created by the non-ideal transition from the nozzle to the control plate. The first oblique shock is observed to remain at the same angle regardless of shock position and voltage. The shock angle is 42° ±1°, which is slightly larger than the theoretical M = 1·5 Mach angle. However, it is within experimental and measurement error and is understood to be a Mach wave. It is believed that the second oblique shock is formed by the presence of localised boundary layer thickening created by fluid injection into the boundary layer through the longitudinal 'slots'. This is a localised effect and therefore the secondary shock appears weaker in the schlieren than the first oblique shock, as seen by the lighter line.

The flow structure is in agreement with the general features of separated SBLI defined by Seddon[22] with a slip line occurring from the triple point separating the higher velocity flow, which has passed through the lambda structure with a leading leg shock angle of 46° ±1°. This region is also seen to have reduced total pressure losses. The schlieren picture gives a triple point height of approximately 26mm, as shown by the abrupt change in shock angle in Fig. 6(a), while the total pressure plots suggest it as 25·5mm, as seen from the total pressure ratio, which rises considerably above the theoretical value.

4.2 Unimorph controlled SBLI

Referring to Figs 6(b) and (c), the angle of the second oblique shock is greater with 'flaps closed' (500V), as the reduced unimorph deflection has decreased fluid injection across the end of the unimorph. This is expected to result in increased mass transfer across the side slots, leading to increased boundary-layer thickening and a stronger shock.

The bottom of the normal recovery shock is seen to bifurcate with a shear layer forming and continuing downstream of the triple point. The angle of the leading shock of the lambda structure, calculated from the schlieren with an accuracy of ±1°, changes from 56·5° ('flaps closed') to 54° ('flaps open'). With 'flaps closed' the orifice area for mass transfer is smaller, producing less mass transfer rate. Furthermore, with 'flaps open' the mass transfer will be more tangential reducing the shock angle.

It is observed, from the total pressure traverses, that the height of the triple point on the centre line, $Z = 0$, is approximately 27·5mm and 30·0mm for 'flaps closed' and 'flaps open' respectively. This trend is expected because 'flaps open' produce a greater level of control, mass transfer and hence smearing of the shock. The increased triple point height, and therefore reduced total pressure loss, proves the concept of active control using 'smart' unimorph flaps. However, the level of control is small due to the small amounts of strain, and hence deflection, achievable by the piezoelectric material. The boundary-layer thickness, as determined from the total pressure traverses for both flap positions, is approximately 16·5mm after the interaction, which is slightly larger than the 14·5mm for zero deflection SBLI, see Fig. 6(a).

The triple point and boundary-layer thickness at $Z = 22$mm, which is 9mm outside of the unimorph control region, is 25mm and 21mm respectively for both flap positions. It is believed that this SBLI is comparable to an uncontrolled SBLI as there is minimal unimorph control effects experienced at this spanwise position. However, the increased boundary layer thickness is believed to be due to the influence of the sidewall boundary layer.

Comparing the results of 'zero deflection' (Fig. 6(a)), 'flaps closed' and 'flaps open' (Figs 6(b) and (c)) we observe the following features: while the total pressures at locations away from the centreline ($Z = 0$) are nearly the same, the total pressure profile on the centreline for the zero deflection case shows higher total pressure recovery as compared to that for the 'closed' and 'open' cases between the triple point and the boundary-layer edge. While at first sight this appears contrary to what is expected, it is the result of the 'stretching' of the region between the higher triple point and the boundary layer in the 'closed' and 'open' cases. This is the result of increased mass transfer when the unimorph flaps are activated.

Unfortunately no measurements could be taken of the actual tip deflection achieved during a wind tunnel run due to the confined area within the sealed plenum chamber. Furthermore, no intrusive measuring system could be used external to the plenum chamber as this would interfere with and change the flow structure over the test section.

4.3 Discrete pressure measurements

Surface pressures were measured at various locations, (Fig. 3(b)), non-dimensionalised with respect to the tunnel upstream stagnation pressure and compared to the 'no control' case, which are shown in Figs 7(a) – (c). A slight pressure rise at the start of the interaction region can be observed in all three figures, produced by the first oblique shock created from boundary-layer thickening due to mass injection across the upstream longitudinal slots. The surface pressures then reduce due to boundary-layer thickening up to the main pressure rise. With zero unimorph flap deflection the pressure rise is approximately uncontrolled, see Fig. 7(a).

With a 500V applied voltage, the 'flaps closed' position, the pressure rise is similar to the 'no control' case, but there are significant differences. The slight pressure at the start of interaction region indicates the foot of the first oblique shock followed by boundary-layer thickening. Furthermore, the pressure rise across the main shock is observed to occur slightly upstream compared to the 'zero deflection' and 'no control' case indicating a larger lambda structure and that an active control effect is produced with 'flaps closed'. That is to say with 500V, the 'flaps closed' position, the unimorphs do not negate the aeroelastic deflection generated by the pressure difference due to the presence of the shock.

It is expected that an increase in the level of control will be achieved with –500V due to an increase unimorph deflection and, therefore, mass flow through the plenum chamber. It is observed from Fig. 7(c) that this is, indeed, the case with the pressure rise across the main shock occurring further upstream compared to the 'zero deflection' and 'flaps closed' case. It is believed that the slight dip observed at $X = -5$mm is the effect of mass injection situated at X= –10mm, which generates a localised region of expansion and possibly a small local separation.

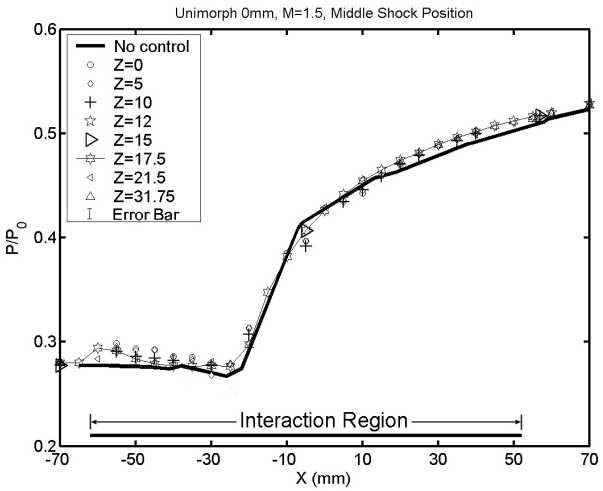
Referring to Figs 7(a) – (c), the surface pressures downstream of the shock position are greater than the 'no control' case' and increase with flap deflection. It is believed that this is due to the lambda structure being located further upstream with flap deflection, shifting the pressure trace proportionally.

4.4 Unimorph control limitation

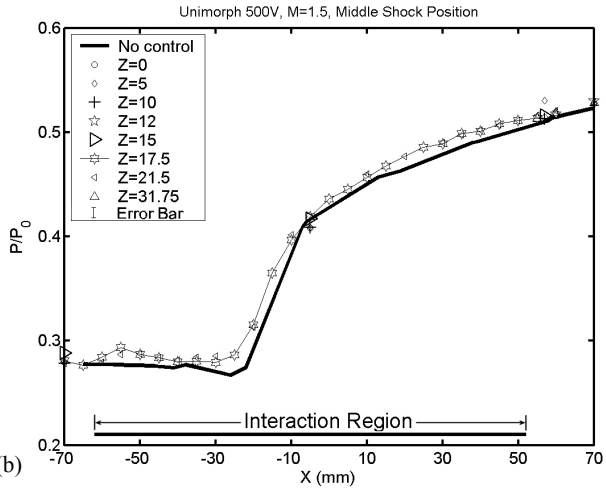
Skin friction measurements were not made during the current study. It may be true that the presence of the unimorph flaps may increase the average skin friction over the control plate and hence drag of the SBLI region. However, it is believed that skin friction will still be less than with passive control using a porous (rough) surface covering a plenum chamber.

The differences between the uncontrolled ('zero deflection') and controlled ('open' and 'closed') cases seem to be quite small with a slight reduction in the adverse pressure gradient, see (Figs 7(a – c)). This is due to the small amounts of unimorph deflection possible, as

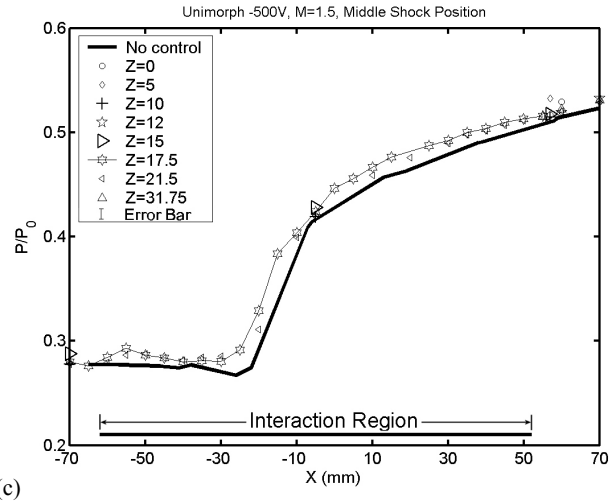
https://doi.org/10.1017/S0001924000000919 Published online by Cambridge University Press



(a)



(b)



(c)

Figure 7. Discrete pressure data of unimorph control with (a) zero deflection, (b) 'closed flaps' (+500V) and (c) 'open flaps' (-500V).

discussed in Sections 3.2, 4.2 and 4.3. It is clear that greater deflection is required for optimal control.[23-25] However, to achieve the deflection required for optimal control, a piezoelectric material with greater strain producing capabilities than currently available is required.[26]

5.0 PIEZOELECTRIC MATERIAL LIMITATIONS

As stated earlier, piezoelectric materials have particular operating limits in terms of temperature, voltage and stress. The chemical composition of the material determines these limits. Operating outside these limits may cause partial or total depolarisation/breakdown of the material and degradation of piezoelectric properties. For these reasons, FEM was used to determine the stresses due to the mechanical and electrical loads at each stage of deflection and in different configurations. However, the piezoelectric 'breakdown' characteristics of the material cannot be fully determined.

6.0 CONCLUSIONS

Active control, in principle, allows optimisation of the interaction by positioning the control region around the original shock position and by controlling mass transfer rates. The present design of substrate flap structure is a trade-off between allowing sufficient mass transfer for control and aeroelastic deflection due to the pressure difference so as to create active control. The resulting structure creates an approximate deflection range of 0 – 0·25mm.

A 500V applied voltage creates a quasi-closed surface minimising mass transfer. This has been labelled controlled – 'flaps closed' case and has similar flow characteristic to the uncontrolled – 'zero deflection' case. However, the presence of longitudinal slots produces continuous passive SBLI control. A –500V applied voltage assists the pressure deflection and is labelled controlled – 'flaps open'. This increased deflection produces a greater level of control, mass transfer and hence greater smearing of the shock. It is observed that the angle of the leading shock of the lambda structure changes from 56·5° ('flaps closed') to 54° ('flaps open'). The increases triple point height with a weaker lambda structure with 'flaps open' reduces total pressure loss, thus proving the concept of active control.

The level of control produced by unimorph flaps is small due to the small amounts of strain, and hence deflection, achievable by the piezoelectric material. It is believed that increased deflection would provide greater control effects tending towards optimisation. However for such piezoelectric flap actuators, a material with greater strain, than presently commercially available, would need to be produced.

REFERENCES

1. GREEN, J.E. Interactions between shock waves and turbulent boundary layers, *Progress in Aero Sci,* 1969, **11,** pp 253-340.
2. ALVI, A. and SETTLES, G.S. Physical model of the swept shock wave boundary-layer interaction flowfield, *AIAA J,* 1992, **30,** (9), pp 2252-2258.
3. ATKIN, C.J. and SQUIRE, L.C. A study of the interaction of a normal shock wave with a turbulent boundary layer at Mach numbers between 1·30 and 1·55, *Eur J Mech B/Fluids,* 1992, **11,** (1), pp 93-118.
4. SETTLES, G.S. and DOLLING, D.S. Swept Shock-Wave/Boundary Layer Interactions, *Progress in Astron and Aeron,* 1992, **141** (SEEBASS A.R. (Ed)), pp 505 - 574.
5. INGER, G.R. Application of a shock-turbulent boundary layer interaction theory in transonic flowfield analysis, AIAA Transonic Perspective Symposium, NASA/Ames Research Center, Moffett Field, California, USA, 18-20 February 1981.

https://doi.org/10.1017/S0001924000000919 Published online by Cambridge University Press

6. KUBOTA, H. and STOLLERY, J.L. An experimental study of the interaction between a glancing shock wave and a turbulent boundary layer, *J Fluid Mech,* 1982, 116, pp 431-458.
7. GIBSON, T.M., BABINSKY, H. and SQUIRE, L.C. Passive control of shock wave/boundary layer interactions, *Aeronaut J,* 2000, pp 124-140.
8. BAHI, L., ROSS, J.M. and NAGAMATSU, H.T. Passive shock wave/boundary layer control for transonic airfoil drag reduction, AIAA 21st Aerospace Sciences Meeting, Reno, NV, USA., January 1983.
9. BABINSKY, H. Control of swept shock wave/turbulent boundary-layer interactions, ISSW22, Imperial College, London, UK, July 18-23 1999.
10. NAGAMATSU, H.T., MITTY, T.J. and NYBERG, G.A. Passive shock wave/boundary layer control of a helicopter rotor airfoil in a contoured transonic wind tunnel, AIAA 25th Aerospace Sciences Meeting, Reno, Nevada, USA, January 1987.
11. NAGAMATSU, H.T., FICARRA, R.V. and DYER, R. Supercritical airofoil drag reduction by passive shock wave/boundary layer control in the Mach number Range ·75 to ·90. AIAA 23rd Aerospace Sciences Meeting, Reno, Nevada, USA, January 1985.
12. RAGHUNATHAN, S. Effects of porosity strength on passive shock-wave/boundary layer control *AIAA J,* 1987, **25,** (5), pp 757-758.
13. RAGHUNATHAN, S. GRAY, J.L. and COOPER, R.K. Effects of inclination of holes on passive shock wave boundary layer control, AIAA 25th Aerospace Sciences Meeting, Reno, Nevada, USA, January 1987.
14. RAGHUNATHAN, S. and MABEY, D.G. Passive shock-wave/boundary layer control on a wall-mounted model, 1987, *AIAA J,* **25,** (2), pp 275-278.
15. RAGHUNATHAN, S. Passive control of shock-boundary layer interaction, *Progress in Aeros Sci,* 1988, *25,* pp 271-296,
16. SAVU, G. and TRIFU, O. Porous airfoils in transonic flow, 1984, *AIAA J,* **22** (7 - Technical Notes), pp 989-991.
17. COULDRICK, J.S., GAI, S., MILTHORPE, J. and SHANKAR, K. Development of 'smart' flap actuators for swept shock wave boundary layer interaction control. Australian International Aerospace Conference, Canberra, Australia, 2001.
18. COULDRICK, J.S., GAI, S., MILTHORPE, J. and SHANKAR, K. Swept shock wave boundary layer interaction control with 'smart' flap actuators, 40th AIAA Aerospace Sciences Meeting & Exhibit, Reno, USA, January 2002.
19. COULDRICK, J.S., SHANKAR, K., GAI, S. and MILTHORPE, J. Design optimisation of 'smart' flap actuators for swept shock wave boundary layer interaction control, 2nd Advances in Structural Engineering and Mechanics, Pusan, Korea, 21-23 August 2002.
20. COULDRICK, J.S., GAI, S., MILTHORPE, J. and SHANKAR, K. Active control of swept shock wave/turbulent boundary layer interactions, *Aeronaut J,* 2004, **108,** (2), pp 93-102.
21. COULDRICK, J.S., SHANKAR, K., GAI, S. and MILTHORPE, J. Design of 'smart' flap actuators for swept shock wave/turbulent boundary layer interaction control, *Struct Eng and Mech: An Inter Journal,* 2003, **16,** (5), pp 519-532.
22. SEDDON, J. The flow produced by interaction of a turbulent boundary layer with a normal shock wave of strength sufficient to cause separation, No. 3502, HMSO ARC, R&M London, March 1960.
23. WOOD, B., LOTH, E. and GEUBELLE, P. Mesoflaps for aeroelastic transpiration for SBLI control, AIAA 37th Aerospace Sciences Meeting, Reno, Nevada, USA, January 1999.
24. LEE, Y., HAFENRICHTER, E.S., ORPHANIDES, M.J., DUTTON, J.C., GRAFTON, W., WILKINS, L.J., MCILWAIN, S.T. and LOTH, E., Experimental study of normal shock wave/turbulent boundary-layer interaction control using the SMART system, 40th AIAA Aerospace Sciences Meeting and Exhibit, Reno, Nevada, USA, 14-17 January 2002.
25. JAIMAN, R.K., LOTH, E. and DUTTON, J.C., Simulations of normal shock-wave/boundary layer interaction control using mesoflaps, 41st AIAA Aerospace Sciences Meeting & Exhibit, Reno, Nevada, USA, 6-9 January 2003.
26. CRAWLEY, E.F. Intelligent structures for aerospace: a technology overview and assessment, *AIAA J,* 1994, **32,** (8), pp 1689-1699.

https://doi.org/10.1017/S0001924000000919 Published online by Cambridge University Press